TECHNISCHE MECHANIK, Band 20, Heft 3, (2000), 275-282
Manuskripteingang: 13. Juli 2000

A Reference Solution for the Numerical Assessment of Refined Plate Theories Including Boundary Layers and Edge Disturbances

J. Meenen

Using a modified Fourier transformation, an analytical solution for the layered plate under plane bending is derived. In contrast to Pagano's solution, arbitrary boundary conditions at the plate edges can be prescribed. Numerical examples for the three-layered plate are presented, and the influence of the material properties on the size of the boundary layer and the predictions of refined plate theories is discussed.

1 Introduction

In the last thirty years, considerable effort has been made to derive plate theories which are suited for layered structures with low transverse shear stiffnesses. In contrast to the classical laminate plate theories which is based on the assumptions of Kirchhoff (Jones, 1975), most of these so-called refined plate theories involve more than three (respectively five) degrees of freedom. Since they allow for a more complex distribution of stresses and strains in the through-thickness direction, they provide better results for composite plates, especially in those cases where significant shear deformations are present (Noor and Burton, 1989).

The assessment of refined plate theories is often performed by a numerical comparison with analytical reference solutions of the three–dimensional theory of linear elasticity. In most cases, a Navier–type solution for the plate strip under plane bending is used, which has been derived for layered isotropic plates by Bufler (Bufler, 1961) and for orthotropic plates by Pagano (Pagano, 1969). Some authors prefer the solution of the rectangular plate with all four edges simply supported (Noor and Burton, 1989).

For the plate strip under plane bending, Pagano's approach leads to an ordinary homogeneous differential equation, whose unknown coefficients are calculated from the boundary conditions on top and bottom of the plate. The prescription of additional boundary conditions at the plate edges is impossible. The same effect can be observed in the Navier solution of the rectangular plate. Since both solutions are based on a Fourier transformation in the in-plane direction(s), they automatically require periodic boundary conditions. These solutions are therefore incapable of modelling the decay of edge disturbances and boundary layers, which can have a significant effect on the accuracy of the results of the refined plate theory (Koiter and Simmonds, 1972). The conclusions drawn from the numerical assessment on the basis of these reference solutions are therefore valid only in those regions of the plate where no boundary layers are present.

In (Meenen and Altenbach, 1998), an analytical reference solution has been derived which is based on a modified Fourier transformation. In contrast to Pagano's approach, it leads to an ordinary inhomogeneous differential equation, whose particular solution is a function of the boundary conditions at the plate edges. Exploiting this extended solution, numerical examples for the three-layered plate are presented and the influence of material properties on the size of the boundary layer is discussed.

2 Basic Equations

For the derivation of the reference solution, the plate strip shown in figure 1 is considered, which consists of different, linear–elastic plies. The plate strip is subjected on top and bottom to a load which is constant in the x_2–direction and which can be described by

$$\sigma_{33}(x_1, h/2) = \sum_{i=1,3,\ldots} q_i^+ \sin(ipx_1) \qquad \sigma_{33}(x_1, -h/2) = \sum_{i=1,3,\ldots} q_i^- \sin(ipx_1)$$

$$\sigma_{13}(x_1, h/2) = \sum_{i=1,3,\ldots} t_i^+ \cos(ipx_1) \qquad \sigma_{13}(x_1, -h/2) = \sum_{i=1,3,\ldots} t_i^- \cos(ipx_1) \tag{1}$$

with $p = \pi/L$ the half wave length.
At the plate edges $x_1 = 0$ and $x_1 = L$, additional boundary conditions are prescribed, which lead to a stress and displacement field symmetric with respect to $x_1 = L/2$. They can be for example

$$\begin{aligned} \sigma_{11}(0, x_3) &= \sigma_{11}^0(x_3) & \sigma_{11}(L, x_3) &= \sigma_{11}^0(x_3) \\ \sigma_{13}(0, x_3) &= \sigma_{13}^0(x_3) & \sigma_{13}(L, x_3) &= -\sigma_{13}^0(x_3) \end{aligned} \tag{2}$$

but boundary conditions in terms of displacements are possible, too.

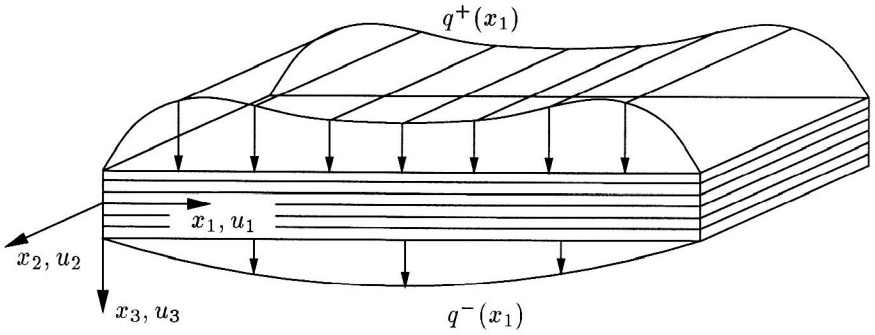

Figure 1: Plate strip

Neighbouring plies of the plate are perfectly bonded together, so that continuity conditions in terms of displacements u_1 and u_3 and interlaminar stresses σ_{33} and σ_{13}

$$\begin{aligned} u_1^k(x_3^{k,+}) &= u_1^{k+1}(x_3^{k,+}) & \sigma_{13}^k(x_3^{k,+}) &= \sigma_{13}^{k+1}(x_3^{k,+}) \\ u_3^k(x_3^{k,+}) &= u_3^{k+1}(x_3^{k,+}) & \sigma_{33}^k(x_3^{k,+}) &= \sigma_{33}^{k+1}(x_3^{k,+}) \end{aligned} \tag{3}$$

hold. It is furthermore assumed that

- the plies of the plate are orthotropic,
- the symmetry axes of the plies are parallel to the coordinate axes x_1, x_2 and x_3 shown in Figure 1,
- the plate is under plane bending in the (x_1, x_3)–plane,
- the displacements and deformations are small,
- the loading on top and bottom of the plate is symmetric with respect to $x_1 = L/2$.

Under these conditions, the three-dimensional equations of elasticity can be reduced to the two-dimensional form

$$\begin{bmatrix} R_{11}^k & R_{13}^k & 0 & -\partial x_1 & 0 \\ R_{13}^k & R_{33}^k & 0 & 0 & -\partial x_3 \\ 0 & 0 & R_{55}^k & -\partial x_3 & -\partial x_1 \\ -\partial x_1 & 0 & -\partial x_3 & 0 & 0 \\ 0 & -\partial x_3 & -\partial x_1 & 0 & 0 \end{bmatrix} \begin{Bmatrix} \sigma_{11} \\ \sigma_{33} \\ \sigma_{13} \\ u_1 \\ u_3 \end{Bmatrix} = 0 \tag{4}$$

where R_{11}, R_{13}, R_{33} and R_{55} are the reduced compliances (compare for example (Altenbach et al., 1996)), and the abbreviations ∂x_1 und ∂x_3 stand for $\partial/\partial x_1$ and $\partial/\partial x_3$.

As shown in (Meenen and Altenbach, 1998) and (Meenen and Altenbach, 1999), an analytical solution of this problem can be found by an integral transformation similar to a Fourier transformation. For this

purpose, the system of equations

$$\phi_i(x_1) := \frac{1}{\sqrt{L}} \mathrm{e}^{\,(jipx_1)} \qquad j = \sqrt{-1} \tag{5}$$

is used, which is orthonormal on the interval $[0, L]$ (Dreszer, 1975)

$$\int_0^L \phi_i(x_1)\overline{\phi_k(x_1)}\mathrm{d}x_1 = \delta_{ik}$$

if all i and k are either even or odd, with $\overline{\phi_k(x_1)}$ the complex conjugate of $\phi_k(x_1)$. The function $f \in \mathrm{L}_2(0, L)$ can then be expanded into the series

$$\sum_{i=-\infty}^{\infty} f^i \phi_i(x_1) \to f(x_1)$$

with the coefficients

$$f^i = \int_0^L f(x_1)\overline{\phi_i(x_1)}\mathrm{d}x_1$$

The expansion of the derivative $f'(x_1) = df(x_1)/dx_1$

$$\sum_{i=-\infty}^{\infty} \tilde{f}^i \phi_i(x_1) \to f'(x_1)$$

leads to the coefficients

$$\tilde{f}^i = \int_0^L f'(x_1)\overline{\phi_i(x_1)}\mathrm{d}x_1 = \left[f(x_1)\overline{\phi_i(x_1)}\right]_0^L + \left(ji\frac{\pi}{L}\right)\int_0^L f(x_1)\overline{\phi_i(x_1)}\mathrm{d}x_1 \tag{6}$$

Assuming that $f(x_1)$ is periodic on the interval $[0, L]$ and using the system with even i, this expansion leads to

$$\tilde{f}^i = \left(ji\frac{\pi}{L}\right)\int_0^L f(x_1)\overline{\phi_i(x_1)}\mathrm{d}x_1 \tag{7}$$

In contrast to this classical formula, the additional terms in equation (6) allow for fulfilling non–periodic boundary conditions. Introducing this transformation into the equations of linear elasticity, and replacing the unknown stresses and displacements by their series expansion leads to the inhomogeneous system of differential equations

$$\begin{bmatrix} R^k_{11} & R^k_{13} & 0 & -(jip) & 0 \\ R^k_{13} & R^k_{33} & 0 & 0 & -\partial x_3 \\ 0 & 0 & R^k_{55} & -\partial x_3 & -(jip) \\ -(jip) & 0 & -\partial x_3 & 0 & 0 \\ 0 & -\partial x_3 & -(jip) & 0 & 0 \end{bmatrix} \begin{Bmatrix} \sigma^i_{11} \\ \sigma^i_{33} \\ \sigma^i_{13} \\ u^i_1 \\ u^i_3 \end{Bmatrix} = \begin{Bmatrix} \hat{u}_1(x_3) \\ 0 \\ \hat{u}_3(x_3) \\ \hat{\sigma}_{11}(x_3) \\ \hat{\sigma}_{13}(x_3) \end{Bmatrix} \tag{8}$$

where the boundary conditions at the plate edges are introduced by the inhomogeneous terms on the right hand side of equation (8). They are calculated from the expression

$$\hat{f}(x_3) := \left[f(x_1, x_3)\overline{\phi_i(x_1)}\right]_0^L \tag{9}$$

In all what follows, it is assumed that the solution is symmetric with respect to $x_1 = L/2$ and that the numbers i are odd. In this case, the four boundary conditions at the plate edges can be reduced to

$$\hat{u}_1(x_3) = 0 \quad \hat{u}_3(x_3) = -\frac{2}{\sqrt{L}} u_3(0, x_3) \quad \hat{\sigma}_{11}(x_3) = -\frac{2}{\sqrt{L}} \sigma_{11}(0, x_3) \quad \hat{\sigma}_{13}(x_3) = 0 \tag{10}$$

Inverting eqs. (8) and replacing σ^i_{11} by

$$\sigma^i_{11}(x_3) = -\frac{1}{R^k_{11}} \left(R^k_{13} \sigma^i_{33}(x_3) - (jip)\, u^i_1(x_3) - \hat{u}_1(x_3) \right) \tag{11}$$

leads to four ordinary inhomogeneous differential equations

$$\begin{aligned}
\mathrm{P}^i \{\sigma^i_{33}(x_3)\} &= \left(j\,(ip)\, R^k_{11} \frac{\mathrm{d}^2}{\mathrm{d}{x_3}^2} - j\,(ip)^3\, R^k_{13} \right) \hat{\sigma}_{11}(x_3) + j\,(ip)^3 \frac{\mathrm{d}}{\mathrm{d}x_3} \hat{u}_3(x_3) \\
\mathrm{P}^i \{\sigma^i_{13}(x_3)\} &= \left(-R^k_{11} \frac{\mathrm{d}^3}{\mathrm{d}{x_3}^3} + (ip)^2\, R^k_{13} \frac{\mathrm{d}}{\mathrm{d}x_3} \right) \hat{\sigma}_{11}(x_3) - (ip)^2 \frac{\mathrm{d}^2}{\mathrm{d}{x_3}^2} \hat{u}_3(x_3) \\
\mathrm{P}^i \{u^i_1(x_3)\} &= \left((ip)^2 \left(R^k_{11} R^k_{33} - {R^k_{13}}^2 \right) - R^k_{11} R^k_{55} \frac{\mathrm{d}^2}{\mathrm{d}{x_3}^2} \right) \hat{\sigma}_{11}(x_3) \\
&+ \left((ip)^2\, R^k_{13} \frac{\mathrm{d}}{\mathrm{d}x_3} - R^k_{11} \frac{\mathrm{d}^3}{\mathrm{d}{x_3}^3} \right) \hat{u}_3(x_3) \\
\mathrm{P}^i \{u^i_3(x_3)\} &= \left(jip(R^k_{11} R^k_{33} - {R^k_{13}}^2 - R^k_{13} R^k_{55}) \frac{\mathrm{d}}{\mathrm{d}x_3} \right) \hat{\sigma}_{11}(x_3) \\
&+ \left(j\,(ip)^3\, R^k_{33} - jip R^k_{13} \frac{\mathrm{d}^2}{\mathrm{d}{x_3}^2} \right) \hat{u}_3(x_3)
\end{aligned} \tag{12}$$

The homogeneous part

$$\mathrm{P}^i \{f(x_3)\} := \left(R^k_{11} \frac{\mathrm{d}^4}{\mathrm{d}{x_3}^4} - (ip)^2 \left(2R^k_{13} + R^k_{55} \right) \frac{\mathrm{d}^2}{\mathrm{d}{x_3}^2} + (ip)^4\, R^k_{33} \right) f(x_3)$$

is identical with the homogeneous differential equation derived by Pagano and Bufler. In the case of antiperiodic boundary conditions,

$$u_3(x_1 = 0, x_3) \equiv 0 \qquad \sigma_{11}(x_1 = 0, x_3) \equiv 0$$

the inhomogeneous parts vanish and the system of equations (12) reduces to Pagano´s solution.

3 Numerical Results for the Three–layered Plate

A particular solution of the system of differential equations can be found if the distribution of the transverse displacement $u_3(0, x_3)$ and the normal stress $\sigma_{11}(0, x_3)$ at the plate edges is known. This is however rarely the case. For the free edge or the clamped edge, an approximate procedure has to be used. In the case of the free edge, the transverse displacement $u_3(0, x_3)$ is replaced by its Fourier transformation in the thickness-direction, the normal stress $\sigma_{11}(0, x_3)$ is identically zero. Apart from the still unknown coefficients of the homogeneous solution, the Fourier coefficients of $u_3(0, x_3)$ are introduced as additional unknowns. The boundary condition $\sigma_{13}(0, x_3) = 0$ is then approximately fulfilled by solving the system of equations

$$2/h^k \int_{-h^k/2}^{h^k/2} \sigma_{13}(0, x^k_3) \mathrm{d}x^k_3 = 0$$

$$2/h^k \int_{-h^k/2}^{h^k/2} \sigma_{13}(0, x^k_3) \cos(2rq^k x^k_3) \mathrm{d}x^k_3 = 0$$

$$2/h^k \int_{-h^k/2}^{h^k/2} \sigma_{13}(0, x_3^k) \sin(2rq^k x_3^k) \mathrm{d}x_3^k = 0 \tag{13}$$

with k the wave number in the thickness direction of the ply. This linear system of equations is completed by the boundary conditions on top and bottom of the plate, the interlaminar conditions of continuity, and an additional equation restricting the rigid body displacement of the plate.

As a numerical example, a plate strip of length $L = 3$ m is modelled, which is subjected to a sinusoidal loading $q^+(x_1) = q_0 \sin(\pi x_1/L)$ with $q_0 = 2.0$ N/m on the upper side. It is composed of three plies with a thickness of 0.1 m, leading to a relative thickness of $h/L = 0.1$. The three plies are transversely–isotropic with the axes of symmetry parallel to the x_1–direction (see Figure 2). The Young's and shear moduli of the inner layer are reduced by a factor of 10 compared to the stiffnesses of the outer layers. The material properties of the outer and the inner layers are listed in Table 1.

The effect of edge disturbances can be investigated by comparing a solution without any boundary layer with results obtained for a well defined edge disturbance. As a reference, the antiperiodic boundary conditions shown in Figure 2 are choosen. From the point of view of a first order shear deformation theory, the antiperiodic boundary conditions are equivalent to those shown in Figure 2b, since they involve the same shear force and bending moment. According to Saint–Venant's principle, the stress distribution in the interior of the plate should be the same. Due to the crack in the upper two layers, the two boundary conditions will however lead to different stress distributions in the vicinity of the edge.

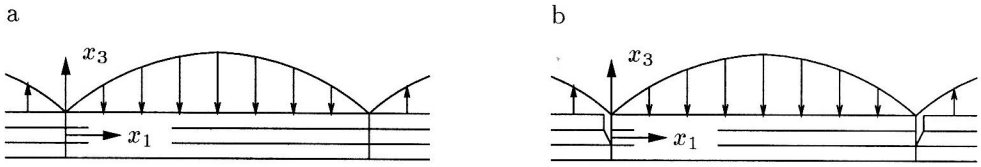

Figure 2: Simply Supported Boundary Conditions. a Antiperiodic Boundary Conditions, b Cracked Edge

	outer layers	inner layers
E_L	$200.0 \cdot 10^9$ N/m^2	$20.0 \cdot 10^9$ N/m^2
E_T	$5.0 \cdot 10^9$ N/m^2	$0.5 \cdot 10^9$ N/m^2
G_{LT}	$5.0 \cdot 10^9$ N/m^2	$0.5 \cdot 10^9$ N/m^2
ν_{LT}	0.25	0.25
ν_{TT}	0.25	0.25

Table 1: Material Properties of the Plies,

The computations were performed for different material properties. Starting from the values listed in Table 1, the parameters E_L, G_{LT}, ν_{LT} and ν_{TT} were varied in the ranges listed in Table 2. The range for ν_{LT} and ν_{TT} was choosen in such a way that the stiffness matrix always remained positive definit (Altenbach et al., 1996).

E_L/E_T	5.0	10.0	20.0	**40.0**	80.0	160.0	
G_{LT}/E_T		0.25	0.5	**1.0**	2.0	4.0	
ν_{LT}	-3.5	-1.0	0.0	**0.25**	1.0	2.0	3.5
ν_{TT}	-0.9	-0.5	0.0	**0.25**	0.5	0.9	

Table 2: Variations of the Material Properties

Figure 3 shows the distribution of the transverse shear stress over the plate thickness x_3 for different

material properties at the plate edge $x_1 = 0$. In all diagrams, the shear stress σ_{13} has been normalized by a factor $(h\pi)/(q_0 L)$. A constant shear stress would therefore have the value 1, since it must hold equilibrium to the loads applied on top of the plate.

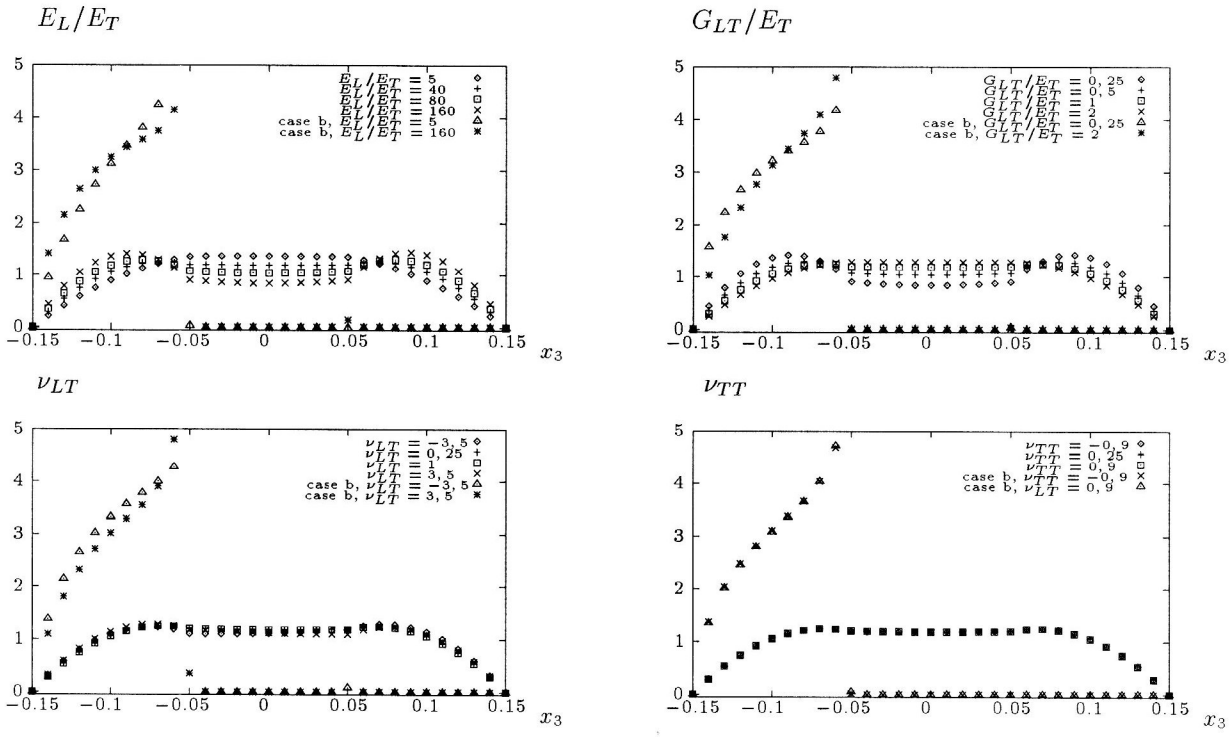

Figure 3: Shear Stresses at the Plate Edges for Different Material Properties

In the diagrams, the results are shown for the periodic as well as for the cracked boundary conditions. As expected, the stress distributions differ significantly. In the case of periodic boundary conditions, the stresses are smoothly distributed over the whole plate thickness, with a maximum in the inner layer, or two maxima in the outer layers and one minimum in the inner layer. The stress distribution is significantly influenced by Young's modulus E_L and the shear modulus G_{LT}. A low Young's modulus $(E_L/E_T = 5)$ or a high shear modulus $(G_{LT}/E_T = 2)$ prevent the existence of two maxima in the outer layers. The Poisson constants ν_{LT} and ν_{TT} do not have a significant influence on the distribution of the edge disturbances.
In the case of the cracked plate, the shear stress vanishes for $x_3 \geq -0.05$ m, i.e. at the two cracked upper layers. The non-zero values for $x_3 = 0.05$ m are numerical errors. The shear stresses are significantly higher than in the case of the undisturbed edge, since the shear stress must assure the overall equilibrium, and a singularity is introduced at the crack tip.

The decay of the edge disturbances introduced by the crack is depicted in the diagrams of figure 4. They show the shear stress in the middle of the upper layer $x_3 = 0.1$ m as a function of the in-plane coordinate x_1. In these diagrams, the shear stress has been normalized by the corresponding value of the reference solution with periodic boundary conditions, at $x_1 = 0$ m and $x_3 = 0.1$ m. The reference solution therefore starts with the value 1 and decays with a cosine function. The shear stress in the disturbed solution starts with the value 0, increases significantly in the vicinity of the edge and converges against the periodic solution in the middle of the plate.

The diagrams clearly show that the Young's modulus E_L has got the biggest influence on the decay of the edge disturbances. Whereas for $E_L/E_T = 5$ the boundary layer has nearly vanished at $x_1 = 2h$, the edge disturbances remain present in nearly the whole plate for $E_L/E_T = 40$. In the same time, the maximum difference between disturbed and undisturbed solution decreases, and the position of the maximum moves towards the middle of the plate. The isotropic plate possesses the highest decay rate,

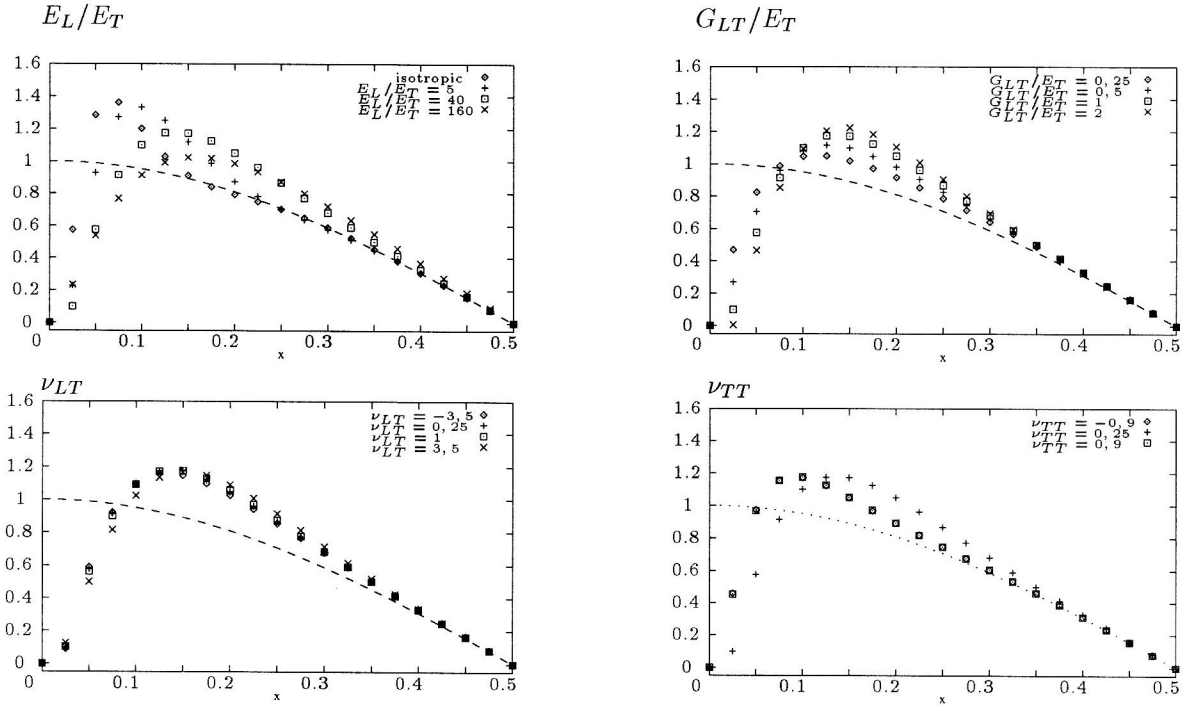

Figure 4: Decay of Edge Disturbances for Different Material Properties

but has the highest maximum, too.
A high shear modulus G_{LT} does only slightly increase the size of the boundary layer. It does however significantly increase the maximum shear stress and move it towards the middle of the plate. An absolutely high ν_{TT} significantly shortens the boundary layer, and Poisson's constant ν_{LT} has nearly any influence on the disturbed solution.

These numerical results agree with the theoretical investigations on Saint–Venant's principle (Horgan, 1972a; Horgan, 1972b; Horgan, 1989; Horgan and Knowles, 1983), which show that the decay rate of edge disturbances is significantly decreased in highly anisotropic materials. Although self–equilibrated edge stresses do not influence the solution in the interior of the plate, Saint–Venant's principle is not applicable in its original form since it states that the boundary layer is of the size of about one plate thickness. In highly anisotropic plates, the size of the boundary layer depends at least on the material properties and on the plate thickness, and can be significantly larger than in the case of an isotropic material.

When analyzing anisotropic plates by means of refined plate theories, it is therefore necessary to identify regions of stress concentrations, induced for example by concentrated forces or edge disturbances. In those regions, refined plate theories with more than five independent unknowns have to be used, since the self–equilibrated edge stresses inducing boundary layer effects cannot be prescribed by the classical resultants "normal force", "shear force" and "bending moment". In most cases, the boundary conditions of the additional resultants of refined plate theories are unknown and must be calculated from a three–dimensional model. They can be explicitly prescribed only in the case of the free or the clamped edge. Refined theories with only five degrees of freedom (Bhimaraddi and Stevens, 1984; di Sciuva, 1984; di Sciuva, 1986; Reddy, 1984) are not capable of describing boundary layer effects, since no information about self–equilibrated edge stresses can be introduced into the solution. They are however preferable for the interior parts of the plate, since they lead to better approximations for layered anisotropic structures than the classical laminate plate theories, without involving more unknowns than necessary.

Acknowledgements

The financial support of the Deutsche Forschungsgemeinschaft (GRK203) is gratefully acknowledged.

Literature

1. Altenbach, H.; Altenbach, J.; Rikards, R.: Einführung in die Mechanik der Laminat- und Sandwichtragwerke. Modellierung und Berechnung von Balken und Platten aus Verbundwerkstoffen. Stuttgart: Deutscher Verlag für Grundstoffindustrie, (1996).

2. Bhimaraddi, A.; Stevens, L. K.: A higher order theory for the free vibration of orthotropic, homogeneous and laminated rectangular plates. Transactions of the American Society of Mechanical Engineers. Journal of Applied Mechanics, 51, (1984), 195–198.

3. Bufler, H.: Der Spannungszustand in einer geschichteten Scheibe. Zeitschrift für Angewandte Mathematik und Mechanik, 41, 4, (1961), 158–180.

4. di Sciuva, M.: A refined transverse shear deformation theory for multilayered anisotropic plates. Meccanica dei solidi, 118, (1984), 279–295.

5. di Sciuva, M.: Bending, vibration and buckling of simply supported thick multilayered orthotropic plates: An evaluation of a new displacement model. Journal of Sound and Vibration, 105, 3, (1986), 425–442.

6. Dreszer, J.: Mathematik Handbuch für Technik und Naturwissenschaft. Zürich: Verlag Harri Deutsch, (1975).

7. Horgan, C. O.: On Saint–Venant's principle in plane anisotropic elasticity. Journal of Elasticity, 2, 3, (1972a), 169–180.

8. Horgan, C. O.: Some remarks on Saint–Venant's principle for transversely isotropic composites. Journal of Elasticity, 2, 4, (1972b), 335–339.

9. Horgan, C. O.: Recent developments concerning Saint–Venant's principle: an update. Applied Mechanics Reviews, 42, 11, (1989), 295–303.

10. Horgan, C. O.; Knowles, J. K.: Recent developments concerning Saint–Venant's principle. Advances in Applied Mechanics, 23, (1983), 179–269.

11. Jones, R. M.: Mechanics of Composite Materials. New York, Washington, Philadelphia, London: Hemisphere Publishing Corporation, (1975).

12. Koiter, W. T.; Simmonds, J. G.: Foundations of shell theory. Technical Report WTHD 40, Laboratorium voor Technische Mechanica Delft, Technische Hoogeschool Delft, (1972).

13. Meenen, J.; Altenbach, H.: Statically equivalent solutions for assessment of refined plate theories. Mechanics of Composite Materials, 34, 4, (1998), 461 –476.

14. Meenen, J.; Altenbach, H.: An extension of Pagano's analytical solution for layered structures to thermal loadings and arbitrary boundary conditions. In: Thermal Stresses '99, Third International Congress on Thermal Stresses (edited by Skrzypek, J. J.; Hetnarski, R. B.), pages 437–440, Cracow University of Technology, Cracow: Bratni Zew, (1999).

15. Noor, A. K.; Burton, W. S.: Assessment of shear deformation theories for multilayered composite plates. Applied Mechanics Reviews, 42, 1, (1989), 1–13.

16. Pagano, N. J.: Exact solutions for composite laminates in cylindrical bending. Journal of Composite Materials, 3, (1969), 398–411.

17. Reddy, J. N.: A simple higher–order theory for laminated composite plates. Transactions of the American Society of Mechanical Engineers. Journal of Applied Mechanics, 51, (1984), 745–752.

Address: Dr.-Ing. Johannes Meenen, U4.26, D-68161 Mannheim. *e-mail:* johannes.meenen@t-online.de